

Preparation and Characterization of C@Fe₃O₄ Supported Pd Magnetic Nanoparticles for Degradation of Dye Wastewater

Xue FANG, Yang WANG*, Xianghong CUI, Shumeng ZHOU, Haijian JIANG, Meihui SONG, Liming YAO, Xiaochen ZHANG

Institute of Advanced Technology, Heilongjiang Academy of Sciences, Harbin, Heilongjiang, China, 150020

<http://doi.org/10.5755/j02.ms.34915>

Received 23 August 2023; accepted 25 December 2023

The core-shell structure Fe₃O₄@C magnetic nanoparticles were synthesized with superparamagnetic Fe₃O₄ nanosphere as a magnetic core, and soluble starch resin as a carbon source via a solvothermal method. Silica-iron oxide and Fe₃O₄@C carriers with a core-shell structure were prepared by carbonization of organic material on the surface of Fe₃O₄ nanoparticles, Fe₃O₄@C supported Pd were processed into magnetic nano-catalysts with core-shell structure, and their catalytic properties were investigated. The resulting environmentally friendly magnetic material can be used to degrade dye wastewater. The structure of magnetic nanoparticles was characterized using TEM, XRD and VSM. The effects of preparation conditions in the structure of the Fe₃O₄@C magnetic nanoparticles were taken out. The results indicate that from XRD, the magnetic nano particles Fe₃O₄@C synthesized of carbon sources have amorphous carbon diffraction peak except for all the characteristic peaks of Fe₃O₄. The saturation magnetization Fe₃O₄, Fe₃O₄@SiO₂ and Fe₃O₄@C – 59.14 emu/g, 49.12 emu/g and 27.95 emu/g, respectively.

Keywords: Fe₃O₄, magnetic nanoparticles, Pd, solvothermal synthesis.

1. INTRODUCTION

With the rapid development of the catalyst industry, more and more attention has been paid to catalysis. In addition to catalytic activity, the selection of catalysts is also receiving more and more attention in terms of economic competitiveness and environmental compatibility. Industrial and academic research on highly efficient and selective catalysts has significantly reduced waste production and treatment costs. However, high costs and difficulty separating and recovering the catalyst are the main problems in liquid-phase reactions [1, 2]. To solve these problems, researchers have developed many methods, such as ionic liquids and supercritical solvents, which have been used to separate catalysts. However, these separation methods have some limitations regarding cost control, efficiency, etc. To solve this problem, magnetic nanomaterials have received significant attention [3, 4]. This is because magnetic nanomaterials can be effectively separated under the action of an intelligent field. Therefore, preparing magnetic catalysts with separation efficiency and selectivity has become the focus of catalysis research [5, 6].

With the rapid development of various manufacturing industries, a large amount of industrial wastewater has been generated, and the discharge of industrial wastewater containing organic dyes has also increased sharply. About 160 million cubic meters of organic dye sewage is discharged into the water environment every year in China [1]. Water pollution caused by organic matter seriously endangers the living environment and the healthy life of human beings. In addition, dye effluent has the characteristics of high color, high content of organic

pollutants, complex composition, large changes in water quality, high biological toxicity, etc., and is difficult for biochemical degradation. Discharging into water bodies will consume dissolved oxygen, disrupt the ecological balance of the water, and endanger the survival of fish and other aquatic organisms. How to deal with such pollutants efficiently has become an increasingly relevant issue, and we need to consider the advances and feasibility of treatment technology. Therefore, dye sewage treatment technology mainly focuses on the following aspects: high efficiency, adaptability and low cost.

Iron, drills, inserts, and other metals are magnetic; common magnetic nanomaterials consist of these metals and metal oxides and complexes. Among these magnetic materials, Fe₃O₄ is the most widely used. It has the advantages of a simple production method, good controllability and stability of particle size, easy dispersion of particles, good biocompatibility, and low toxicity to living beings; it has many special properties, especially catalytic activity, which are different from other solid particles and have great application potential in many fields. Many methods exist to prepare nano-magnetic Fe₃O₄ materials [7, 8]. According to the state of reactants, there are mainly wet and dry methods; according to the type of preparation, there are physical, chemical, and comprehensive methods. Chemical coprecipitation, sol-gel, water/solvothermal, microemulsion, high-temperature decomposition, and template methods are widely used [8–10].

In this research magnetic Fe₃O₄ nanoparticles were synthesized from ferric chloride hexahydrate by chemical precipitation and solvothermal synthesis and then coated

*Corresponding author. Tel.: 13624510365.
E-mail: xiaoxue@jathas.ac.cn (Y. Wang)

with a carbon layer by hydrothermal method using soluble starch as a carbon source. Magnetic $\text{Fe}_3\text{O}_4@\text{C}$ nanocatalysts were prepared by loading metal components onto the processed supports and fixing the metal components on the surface of the supports with sodium borohydride.

2. EXPERIMENTAL

2.1. Experimental materials

In the experiment, we used ferric chloride produced by Sinopharm Chemical Reagent Co., Ltd.; Ferric chloride and sodium borohydride. Soluble starch and palladium chloride produced by Sinopharm Chemical Reagent Co., Ltd. We purchased polybutylene glycol (AR) from Tianjin Kemi Chemical Reagent Co., Ltd.; Ammonia; (AR) ethanol and ethyl orthosilicate (AR). The water used in the experiment was distilled.

2.2. Synthesis of Fe_3O_4

Synthesis of Fe_3O_4 by chemical precipitation included: chlorides containing iron ions (Fe^{3+} and Fe^{2+}) were mixed in a mass ratio of 1:2. Then, a mixed solution was formed, which was dropped at a rate of 10 mL/min using NaOH solution as precipitant; the pH was controlled in the range of 5–6, and the hybrid systems were stirred at 500 r/min speed at 30 °C temperature, and the precipitate was washed and dried after the synthesis reaction. Finally, magnetic Fe_3O_4 nanoparticles were obtained, and the particle size of the obtained Fe_3O_4 nanoparticles was studied.

Synthesis of Fe_3O_4 by solvothermal: Magnetic Fe_3O_4 nanoparticles were prepared by solvothermal according to the method described in [11, 12]. With stirring, 1.3 g $\text{FeCl}_3 \cdot 6\text{H}_2\text{O}$, 2.4 g sodium acetate, 0.4 g trisodium citrate and 6.0 g polyvinylpyrrolidone-K30 (PVP-K30) were dissolved in 100 mL glycol. The homogeneous yellow solution obtained was transferred to a 100 mL Teflon-lined stainless steel autoclave. The autoclave was sealed and heated to 200 °C. After 10 hours of heating, the autoclave was naturally cooled to room temperature. The obtained black magnetite particles were separated with a permanent magnet, washed with deionized water and ethanol, and dried in a vacuum at 60 °C for 24 hours.

2.3. Synthesis of $\text{Fe}_3\text{O}_4@\text{SiO}_2$

0.1 g of the prepared ferrosferric oxide nanoparticles was ultrasonically dispersed in a mixture of 35 mL ethanol and 10 mL water, and 1 mL ammonia was added to the system with mechanical stirring, 50 mL ethyl orthosilicate was injected and mechanically stirred for 8 h at room temperature. After the reaction, the brown solution was magnetically separated and washed three times with deionized water to remove the unreacted raw materials and impurities, and the $\text{Fe}_3\text{O}_4@\text{silica}$ complex was obtained.

2.4. Synthesis of $\text{Fe}_3\text{O}_4@\text{C}$

4.0 g of soluble starch and 2.0 g of polyethylene glycol were mixed with 160 ml of distilled water in a beaker under mechanical stirring at room temperature for 3 hours until the starch and polyethylene glycol were uniformly dispersed. Then, the Fe_3O_4 nanoparticles were added for 30 minutes under ultrasound to disperse 0.2 g of the prepared synthetic

Fe_3O_4 . The mixed liquid was poured into the stainless steel reaction lid lined with a special gas kite and sealed. The mixture was heated to 180 °C in a drying oven, kept at a temperature for 9 hours, and then cooled to room temperature. After opening the high-pressure reactor, the reaction of the black liquid could be seen in the beaker and washed with ethanol; all the products are separated from the black products by using a magnetic field.

The black product was cleaned with deionized water and ultrasonicated for 15 minutes. After magnetic separation 3–5 times, the black product was washed with ethanol, ultrasound, and magnetic separation. After the surface of the product was dried in a vacuum drying box at 60 °C for 12 hours and stored as a reserve [13, 14].

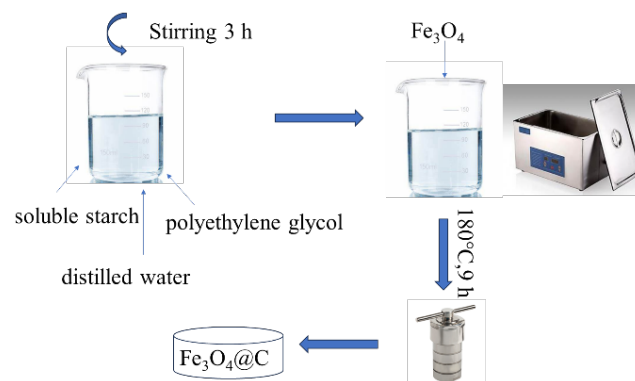


Fig. 1. Synthesis of $\text{Fe}_3\text{O}_4@\text{C}$

2.5. Synthesis of $\text{Fe}_3\text{O}_4@\text{C}/\text{Pd}$

1 g of $\text{Fe}_3\text{O}_4@\text{C}$ was added to 100 ml of deionized water and then sonicated for 5 minutes at room temperature to disperse $\text{Fe}_3\text{O}_4@\text{C}$. The liquid was dispersed into a round bottom flask, 1 mL of 0.5 mg/mL chlorinating solution was added with vigorous stirring for 12 hours at room temperature. 0.15 g of sodium borohydride was weighed, it was dissolved in 45 mL of ethanol, it was dispersed under ultrasound, and it was added to the stirred liquid. The stirring was stopped after stirring for 2 hours. After stratification, the liquid was rinsed alternately with deionized water and ethanol and left to stand. After the product's surface is dried, the beaker with the product is placed in a vacuum drying oven and dried at 60 °C for 12 hours.

2.6. Characterization methods

The surface topography of the sample was studied by JEOL JSM-6700F scanning electron microscope (SEM) with a primary electron energy of 3 kV. X-ray diffraction (XRD) data was collected using the X'Pert PRO diffractometer. The thermogravimetric analyzer data was collected using a TG209F3 thermogravimeter from NETZSCH, Germany.

3. RESULTS AND DISCUSSION

The SEM images of Fe_3O_4 nanoparticles prepared by chemical precipitation and solvothermal methods, respectively, are shown in Fig. 2. However, the preparation process is tedious, and the dispersion of the Fe_3O_4 nanoparticles was not as good as that of the Fe_3O_4

nanoparticles prepared by the solvothermal method in Fig. 2 b. The crystallization and crystal growth of Fe_3O_4 in solvothermal synthesis is an extremely complex process.

Therefore, Fe_3O_4 nanoparticles prepared by the solvothermal method were chosen as the core of magnetic composites in the following research.

The pH of the reaction system, temperature, heating rate, and reaction time greatly influence the nanoparticles' size, morphology, and magnetic properties. The advantage of solvothermal synthesis of iron(III) oxide nanoclusters is that they can be formed directly, avoiding the calcination process required by conventional liquid phase synthesis methods and thus largely avoiding the formation of agglomerations [11, 12]. Fig. 1 c shows $\text{Fe}_3\text{O}_4@\text{C}/\text{Pd}$ prepared chemically, and Fig. 1 d shows $\text{Fe}_3\text{O}_4@\text{C}/\text{Pd}$ prepared by solvothermal method. Compared with pure Fe_3O_4 , the surface of Fig. 1 c and d were significantly rougher, but the $\text{Fe}_3\text{O}_4@\text{C}/\text{Pd}$ prepared by the two methods were not significantly different from the surface morphology.

Fe_3O_4 nanoparticles prepared by the solvothermal method and $\text{Fe}_3\text{O}_4@\text{C}/\text{Pd}$ prepared by the solvothermal method were selected for the elemental concentration. The EDS analysis in Fig. 3 a shows that oxygen mass fraction of 25.15 wt.% and iron mass fraction of 74.85 wt.%. Fig. 3 b shows the carbon mass fraction of 19.57 wt.%, Pd mass fraction of 0.28 wt.%, oxygen mass fraction of 29.56 wt.%, and iron mass fraction of 50.59 wt.%.

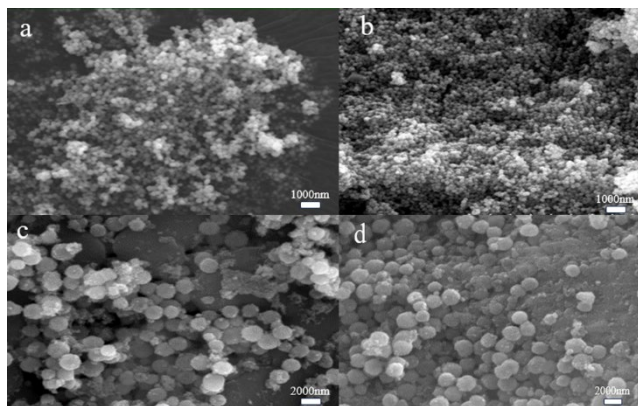


Fig. 2. SEM images: a – Fe_3O_4 by chemical precipitation; b – Fe_3O_4 by solvothermal methods; c – $\text{Fe}_3\text{O}_4@\text{C}/\text{Pd}$ by chemical precipitation; d – $\text{Fe}_3\text{O}_4@\text{C}/\text{Pd}$ by solvothermal methods

The XRD patterns of Fe_3O_4 , $\text{Fe}_3\text{O}_4@\text{C}$, and $\text{Fe}_3\text{O}_4@\text{C}/\text{Pd}$ are shown in Fig. 4. Many characteristic peaks can be seen in the XRD patterns. The diffraction patterns of these nanoparticles are independent of each other. Moreover, there are still clear diffraction peaks after coating with a carbon layer, which shows that these magnetic nanoparticles have perfect crystal shapes. As shown in Fig. 4, the angles of diffraction are 30.1° , 35.3° , 43.1° , 56.8° , 62.4° . There are clear diffraction peaks (220), (311), (422), (511), and (440), indicating that the three types of nanoparticles have a cubic structure. Compared with the characteristic diffraction patterns of the Fe_3O_4 , $\text{Fe}_3\text{O}_4@\text{C}$ shell-core structure, the intensity of the characteristic peaks of the XRD patterns of the $\text{Fe}_3\text{O}_4@\text{C}$ shell-core structure is weaker, which is due to the influence of the C-layer of the Fe_3O_4 coating.

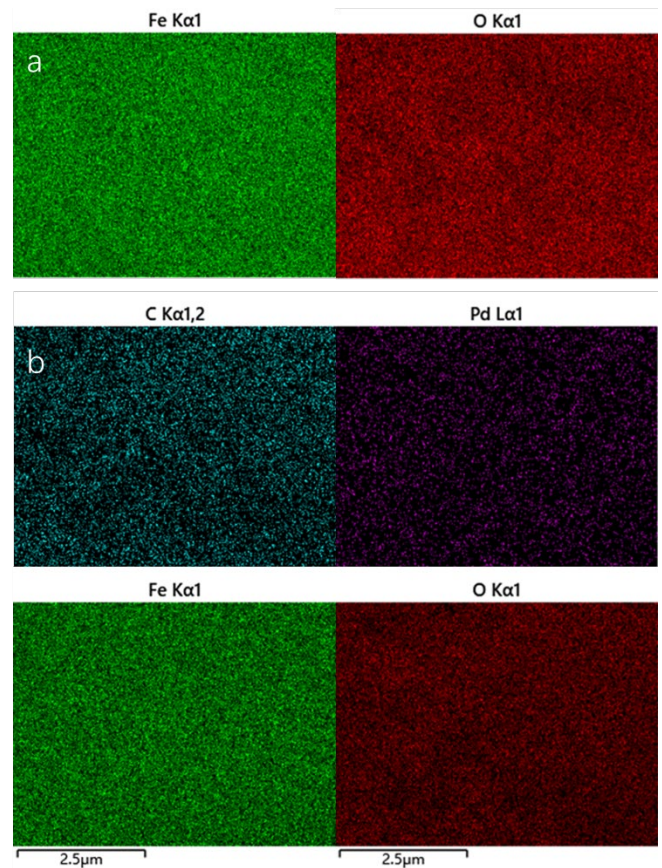


Fig. 3. EDS images of Fe_3O_4 -and $\text{Fe}_3\text{O}_4@\text{C}/\text{Pd}$ -b

It has been demonstrated that the fabricated samples contain both Fe_3O_4 and C. The magnetization curves of superparamagnetic Fe_3O_4 nanospheres by chemical precipitation and solvothermal methods, $\text{Fe}_3\text{O}_4@\text{SiO}_2$ and $\text{Fe}_3\text{O}_4@\text{C}$ magnetic nanoparticles are shown in Fig. 5.

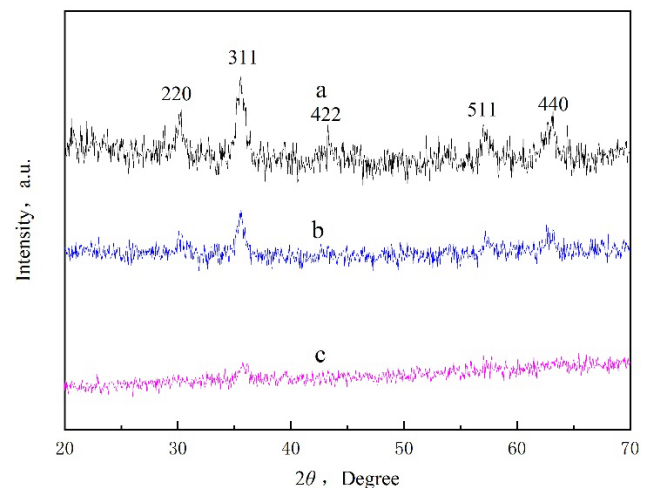


Fig. 4. XRD images: a – Fe_3O_4 ; b – $\text{Fe}_3\text{O}_4@\text{C}$; c – $\text{Fe}_3\text{O}_4@\text{C}/\text{Pd}$

All curves show nonlinear and reversible characteristics without hysteresis, suggesting superparamagnetic behavior. The value of saturation magnetization (M_s) of Fe_3O_4 is 59.14 emu/g. Although the magnetism is weak after coating $\text{Fe}_3\text{O}_4@\text{SiO}_2$ and the carbon shell, the saturation magnetization values of $\text{Fe}_3\text{O}_4@\text{SiO}_2$ and $\text{Fe}_3\text{O}_4@\text{C}$ are 49.12 emu/g and 27.95 emu/g, respectively, which fully satisfies the magnetic

separation requirements and protects $\text{Fe}_3\text{O}_4@\text{SiO}_2$ and $\text{Fe}_3\text{O}_4@\text{C}$ from agglomeration while providing better dispersibility.

Magnetism is an important physical parameter of all magnetic ferrite materials. For Fe_3O_4 particles, the main concern was the strength of the magnetic response (saturation magnetization, Ms). The saturation magnetization means that the magnetic moment of the magnetic domain tends in the same direction as the external magnetic field under the action of the external magnetic field, forming a magnetization vector. Magnetization increases as the external magnetic field gradually increases until it reaches the maximum value. As can be seen from Fig. 5, the material exhibits paramagnetism.

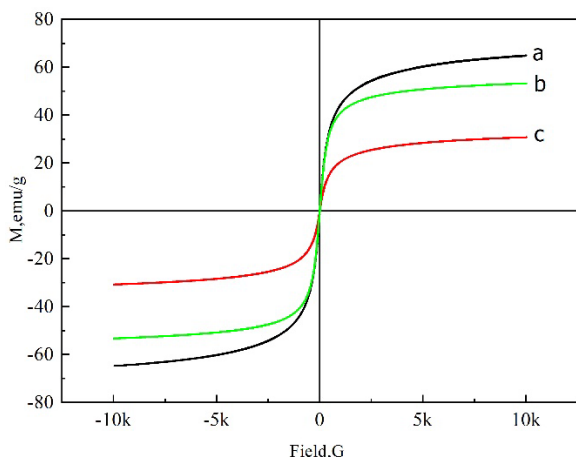


Fig. 5. VSM of: a – Fe_3O_4 ; b – $\text{Fe}_3\text{O}_4@\text{SiO}_2$; c – $\text{Fe}_3\text{O}_4@\text{C}$

The saturation magnetization strength decreases because the increase in shell thickness makes magnetic field separation difficult [13, 14].

To better observe the magnetic response of the $\text{Fe}_3\text{O}_4@\text{C}/\text{Pd}$ composites, the samples were dispersed in ethanol, and the photos were taken before and after applying the magnetic field (Fig. 6). In Fig. 6 a, the composites are uniformly dispersed in the ethanol solution before the application of the magnetic field. In Fig. 6 b, it can be seen that the sample aggregates on the side near the magnet after applying the magnetic field, which intuitively shows that the synthesized $\text{Fe}_3\text{O}_4@\text{C}/\text{Pd}$ composites have some magnetic response.

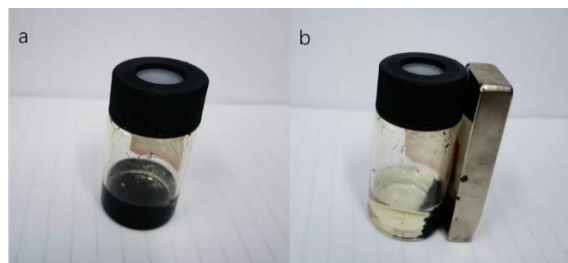


Fig. 6. Photographs of the $\text{Fe}_3\text{O}_4@\text{C}/\text{Pd}$ composites ethanol dispersion before and after applying a magnetic field: a – without an applied magnetic field; b – with an applied magnetic field

Sodium borohydride reduced methylene blue (MB) was used as a reference system to study the catalytic activity of $\text{Fe}_3\text{O}_4@\text{C}/\text{Pd}$. Fig. 7 shows the UV–Vis pattern of this process, the initial methylene blue dye solution Fig. 7 a; the

methylene blue dye solution after reaction for 8 h without $\text{Fe}_3\text{O}_4@\text{C}/\text{Pd}$ composites Fig. 7 b; the methylene blue dye solution after reaction for 10 min in the presence of $\text{Fe}_3\text{O}_4@\text{C}/\text{Pd}$ composites Fig. 7 c. The initial methylene blue solution is dark blue and the maximum absorption wavelength of the solution appears at 665 nm (Fig. 7 a). After adding a certain amount of sodium borohydride, after 8 h of the reaction, the absorption intensity at the maximum absorption wavelength decreased but did not completely disappear, and the color of the solution changed from dark blue to light blue (Fig. 7 b). This shows that in the absence of a catalyst, methylene blue solution is difficult to reduce. When 2.0 mg $\text{Fe}_3\text{O}_4@\text{C}/\text{Pd}$ was added to the system, the absorption intensity completely disappeared (Fig. 7 c) and the color of the solution changed to colorless within 10 min. Based on the above UV–Vis analysis, it can be concluded that the $\text{Fe}_3\text{O}_4@\text{C}/\text{Pd}$ complex has excellent catalytic properties.

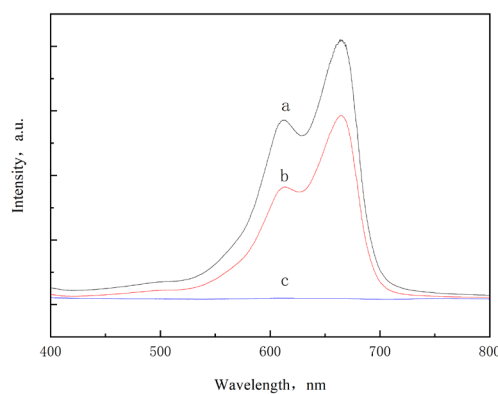


Fig. 7. a – Vis spectra: the initial methylene blue dye solution; b – the methylene blue dye solution after reaction for 8 h without $\text{Fe}_3\text{O}_4@\text{C}/\text{Pd}$ composites; c – the methylene blue dye solution after reaction for 10 min in the presence of $\text{Fe}_3\text{O}_4@\text{C}/\text{Pd}$ composites

The performance of the $\text{Fe}_3\text{O}_4@\text{C}/\text{Pd}$ catalyst for recycling is shown in Fig. 8. The selectivity of the 20 reactions is constant and remains at 100 %. However, as the number of reactions increases, the mass of the catalyst decreases, possibly due to the loss of the catalyst during the separation and washing process or the loss of the supported Pd during the recycling process, which also decreases the yield of the reaction. Overall, $\text{Fe}_3\text{O}_4@\text{C}/\text{Pd}$ shows good recycling performance and can be reused.

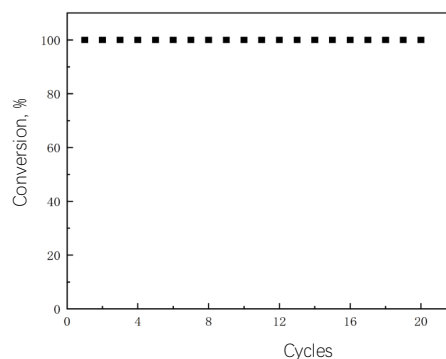


Fig. 8. The conversion of the catalyst after 20 catalytic reaction cycles

4. CONCLUSIONS

Magnetic Fe₃O₄ nanoparticles were prepared by solvothermal synthesis from ferric chloride hexahydrate and coated with silica and carbon, respectively. The Fe₃O₄@C/Pd magnetic nano-catalyst was prepared by loading noble metal components onto the processed Fe₃O₄@C support and fixing the noble metal components on the surface of the support by sodium borohydride reduction. The XRD results shows that the crystal structure of Fe₃O₄@C was not changed after coating. The noble metal component Pd is present in the Fe₃O₄@C/Pd catalyst. The VSM diagram shows that a magnetic field can separate the magnetic Fe₃O₄@C/Pd nano-catalyst, and both the magnetic and coercive forces are zero. The Fe₃O₄@C/Pd composites are used as catalysts to degrade dyes in wastewater, which is not only efficient, fast, environmentally friendly, and easy to recycle.

REFERENCES

1. Yao, T.J., Cui, T.Y., Fang, X., Yu, J., Cui, F., Wu, J. Preparation of Yolk/shell Fe₃O₄@polypyrrole Composites and Their Applications as Catalyst Supports *Chemical Engineering Journal* 225 2013: pp.230–236. <https://doi.org/10.1016/j.cej.2013.02.026>
2. Shi, D., Y, H., Ji, S.F., Jiang, S., Liu, X.F., Zhang, D.N. Preparation and Characterization of Core-shell Structure Fe₃O₄@C Magnetic Nanoparticles *Procedia Engineering* 102 2015: pp. 1555–1562. <https://doi.org/10.1016/j.proeng.2015.01.291>
3. Crooks, R.M., Zhao, M.Q., Sun, L., Chechik, L., Yeung, L.K. Dendrimer-encapsulated Metal Nanoparticles: Synthesis, Characterization, and Applications to Catalysis *Journal of Chemical Research* 34 (3) 2001: pp.181–190. [https://doi.org/10.1002/\(SICI\)15214095\(199903\)11:33.0.CO;2-7](https://doi.org/10.1002/(SICI)15214095(199903)11:33.0.CO;2-7)
4. Liu, W.L., Chuang, Y.C., Hsu, I.J., Cheng, C.M., Huang, C.C. Magnetic Responsive Release of Nitric Oxide from an MOF-Derived Fe₃O₄@PLGA Microsphere for the Treatment of Bacteria-Infected Cutaneous Wound *ACS Applied Materials and Interfaces* 14 (5) 2022: pp. 6343–6357. <https://doi.org/10.1021/acsami.1c20802>
5. Zhang, W.J. A Review of the Electrochemical Performance of Alloy Anodes for Lithium-ion Batteries *Journal of Power Sources* 196 (1) 2011: pp. 13–24. <https://doi.org/10.1002/chem.201102719>
6. Amadei, I., Panero, S., Scrosati, B., Cocco, G., Schiffini, L. The Ni₃Sn₄ Intermetallic as a Novel Electrode in Lithium Cells *Journal of Power Source* 143 (1) 2005: pp.227–230. <https://doi.org/10.1007/s10973-014-4122-7>
7. Mukaibo, H., Momma, T., Shacham-Diamand, Y., Kodaira, M. In Situ Stress Transition Observations of Electrodeposited Sn-Based Anode Materials for Lithium-Ion Secondary Batteries *Electrochemical and Solid-State Letters* 10 (3) 2007: pp. 27–30. <https://doi.org/10.1039/C5RA18756G>
8. Fang, X., Su, G.M., Song, M.H., Jiang, H.J., Cui, X.H., Zhang, X.C., Chen, M.Y. Preparation of Polyimide@Polypyrrole/Palladium Hollow Composites with Applications in Catalysis *Materials Science* 27 2021: pp.192–196. <https://doi.org/10.1016/j.polymer.2021.07.008>
9. Meng, F.B., Zhao, R., Zhan, Y.Q., Lei, Y.J., Zhong, J.C., Liu, X.B. One-step Synthesis of Fe-phthalocyanine/Fe₃O₄ Hybrid Microspheres *Materials Letters* 65 2011: pp.264–267. <https://doi.org/10.1016/j.matlet.2010.09.075>
10. Trchová, M., Šeděnková, I., Konyushenko, E.N. Evolution of PANI Nanotubes: Oxidation of Aniline in Water *Journal of Physical Chemistry B* 110 (19) 2016: pp. 9461–9468. <https://doi.org/10.1021/jp057528g>
11. Nordlinder, S., Nyholm, L., Torbjörn Gustafsson, A., Edstrom, K. Lithium Insertion into Vanadium Oxide Nanotubes: Electrochemical and Structural Aspects *Chemistry of Materials* 18 (18) 2005: pp. 495–497.
12. Jiao, F., Shaju, K.M., Bruce, P.G. Synthesis of Nanowire and Mesoporous Low-temperature LiCoO₂ by a Post-templating Reaction *Cheminform* 36 (51) 2005: pp.6550–6555. <https://doi.org/10.1016/j.mtcomm.2014.08.001>
13. Shao, M.F., Ning, F.Y., Zhao, J.W., Wei, M., Evans, D.G., Duan, X. Hierarchical Layered Double Hydroxide Microspheres with Largely Enhanced Performance for Ethanol Electrooxidation *Chemical Society Reviews* 41 2012: pp. 1071–1077. <https://doi.org/10.1002/adfm.201202825>
14. Todorov, R., Lozanova, V., Knotek, P., Cernokova, E., Vitek, M. Microstructure and Ellipsometric Modelling of the Optical Properties of Very Thin Silver Films for Application in Plasmonics *Thin Solid Films* 628 (30) 2017: pp. 22–30. <https://doi.org/10.1016/j.tsf.2017.03.0>



© Fang et al. 2024 Open Access This article is distributed under the terms of the Creative Commons Attribution 4.0 International License (<http://creativecommons.org/licenses/by/4.0/>), which permits unrestricted use, distribution, and reproduction in any medium, provided you give appropriate credit to the original author(s) and the source, provide a link to the Creative Commons license, and indicate if changes were made.